Open access • Journal Article • DOI:10.1111/GCB.13168

Variability and evolution of global land surface phenology over the past three decades (1982–2012) — Source link

Irene Garonna, Rogier de Jong, Michael E. Schaepman

Institutions: University of Zurich

Published on: 01 Apr 2016 - Global Change Biology (Wiley-Blackwell Publishing, Inc.)

Topics: Land cover, Biome and Climate change

Year: 2016

Variability and evolution of global land surface phenology over the past three decades (1982-2012)

Garonna, Irene ; de Jong, Rogier ; Schaepman, Michael E

Abstract: Monitoring Land Surface Phenology (LSP) is important for understanding both the responses and feedbacks of ecosystems to the climate system, and for representing these accurately in terrestrial biosphere models. Moreover, by shedding light on phenological trends at a variety of scales, LSP has the potential to fill the gap between traditional phenological (field) observations and the large-scale view of global models. In this study, we review and evaluate the variability and evolution of satellite-derived Growing Season Length (GSL) globally and over the past three decades. We used the longest continuous record of Normalized Difference Vegetation Index (NDVI) data available to date at global scale to derive LSP metrics consistently over all vegetated land areas and for the period 1982-2012. We tested GSL, Start- and End-Of Season metrics (SOS and EOS, respectively) for linear trends as well as for significant trend shifts over the study period. We evaluated trends using global environmental stratification information in place of commonly used land cover maps to avoid circular findings. Our results confirmed an average lengthening of the growing season globally during 1982-2012 – averaging 0.22-0.34 days/year, but with spatially heterogeneous trends. 13-19% of global land areas displayed significant GSL change, and over 30% of trends occurred in the boreal/alpine biome of the Northern Hemisphere, which showed diverging GSL evolution over the past 3 decades. Within this biome, the "Cold and Mesic" environmental zone appeared as an LSP change hotspot. We also examined the relative contribution of SOS and EOS to the overall changes, finding that EOS trends were generally stronger and more prevalent than SOS trends. These findings constitute a step towards the identification of large-scale phenological drivers of vegetated land surfaces, necessary for improving phenological representation in terrestrial biosphere models.

DOI: https://doi.org/10.1111/gcb.13168

Originally published at:
Garonna, Irene; de Jong, Rogier; Schaepman, Michael E (2016). Variability and evolution of global land surface phenology over the past three decades (1982-2012). Global Change Biology, 22(4):1456-1468.
DOI: https://doi.org/10.1111/gcb.13168

Received Date : 14-Jul-2015
Accepted Date : 24-Oct-2015
Article type : Primary Research Articles

TITLE PAGE

i. Title:

Variability and evolution of global land surface phenology over the past three decades (1982-2012)

ii. Running head

Phenology of global land surfaces (1982-2012)

iii. List of authors

Garonna, I.[a], De Jong, R.[a], Schaepman, M.E.[a]

iv. Institute of origin

[a] Remote Sensing Laboratories, Department of Geography, University of Zurich, Winterthurerstrasse 190, 8057 Zurich, Switzerland

v. Corresponding author

Irene Garonna, irene.garonna@geo.uzh.ch, tel. +41-44-6355215

vi. Keywords

land surface phenology, $GIMMS_{3g}$, vegetation activity, growing season length, spring and autumn phenology

This article has been accepted for publication and undergone full peer review but has not been through the copyediting, typesetting, pagination and proofreading process, which may lead to differences between this version and the Version of Record. Please cite this article as doi: 10.1111/gcb.13168

vii. Type of paper

Primary Research Article

ABSTRACT

Monitoring Land Surface Phenology (LSP) is important for understanding both the responses and feedbacks of ecosystems to the climate system, and for representing these accurately in terrestrial biosphere models. Moreover, by shedding light on phenological trends at a variety of scales, LSP has the potential to fill the gap between traditional phenological (field) observations and the large-scale view of global models.

In this study, we review and evaluate the variability and evolution of satellite-derived Growing Season Length (GSL) globally and over the past three decades. We used the longest continuous record of Normalized Difference Vegetation Index (NDVI) data available to date at global scale to derive LSP metrics consistently over all vegetated land areas and for the period 1982-2012. We tested GSL, Start- and End-Of Season metrics (SOS and EOS, respectively) for linear trends as well as for significant trend shifts over the study period. We evaluated trends using global environmental stratification information in place of commonly used land cover maps to avoid circular findings.

Our results confirmed an average lengthening of the growing season globally during 1982-2012 – averaging 0.22-0.34 days/year, but with spatially heterogeneous trends. 13-19% of global land areas displayed significant GSL change, and over 30% of trends occurred in the boreal/alpine biome of the Northern Hemisphere, which showed diverging GSL evolution over the past 3 decades. Within this biome, the “Cold and Mesic” environmental zone appeared as an LSP change hotspot. We also examined the relative contribution of SOS and EOS to the overall changes, finding that EOS trends were generally stronger and more prevalent than SOS trends. These findings constitute a step towards the identification of

large-scale phenological drivers of vegetated land surfaces, necessary for improving phenological representation in terrestrial biosphere models.

INTRODUCTION

Monitoring vegetation phenology is not only important to understand the response of vegetation to a changing climate, but also to determine the feedback mechanisms that vegetation response may generate on the climate itself (Cleland *et al.*, 2007; Morisette *et al.*, 2009; Peñuelas *et al.*, 2009). For instance, the timing and duration of vegetation activity throughout a year are central to the understanding of the variability and distribution of the terrestrial carbon sink, and the recent increase in land carbon uptake has been linked to vegetation phenology changes, in addition to CO_2 and land management effects (Schimel *et al.*, 2001; Sitch *et al.*, 2015).

Aside from this key role vegetation phenology plays in the carbon cycle, it is also important for modulating the intra-annual dynamics of albedo, surface roughness and water fluxes (among others). Thus, vegetation phenology is recognized as a fundamental process of biosphere-atmosphere interactions within coupled climate models (Richardson *et al.*, 2013). However, accurately representing phenology in terrestrial biosphere models remains a challenge (Richardson *et al.*, 2012) for a number of reasons, amongst which are the wide inter-specific and spatial variations in phenological changes that exist at plant level (Ibañez *et al.*, 2010), and our limited knowledge of the physical processes that initiate leaf onset and senescence (Arora & Boer, 2005). Thus, there is a need to improve our understanding of the seasonality of vegetation activity at large scales (Richardson *et al.*, 2012). Large-scale phenological data may allow us to quantify the phenological responses to climate and vice versa, and thus provides the potential to bridge the gap between plant-level and modelled phenological research (Morisette *et al.*, 2009).

The existing records of satellite-derived Vegetation Indices (VIs) provide an opportunity to retrospectively derive information about the phenology of vegetated land surfaces – and have given rise to the field of Land Surface Phenology (LSP; (Reed *et al.*, 2003). In recent years, LSP research has increased considerably: for instance, the number of yearly publications on LSP increased ten-fold in 10 years (2004-2014) (*Scopus,* October 2015*,* data not shown). Methodologies of varying complexity have been put forward to derive LSP descriptors such as Start-, End- and Length of the Growing Season (SOS, EOS and GSL, respectively) from VI time series, and commonly used approaches include threshold-based, derivative-based , and model-fitting methods (for a survey of methods, see (Reed *et al.*, 1994; de Beurs & Henebry, 2010). The range of methodologies used contributes to the variation in trends reported, and the variation in LSP indicators and remote-sensing datasets used constitutes a challenge to comparing different studies.

Figure 1 presents reported estimates of long-term change (10 years or more) in SOS, EOS and GSL in large-scale (at least continental) latitudinal LSP studies. Generally the direction of large-scale LSP change is in agreement between studies: results generally point to a lengthening of the growing season associated with both SOS advance and EOS delay, but quantitative estimates related to large-scale trends vary considerably between studies (Figure 1). In particular, there is inter-decadal variation in the trends found and several recent studies have revealed the important contribution of changing senescence to overall GSL trends (Jeong *et al.*, 2011; Zhao *et al.*, 2012; Zhu *et al.*, 2012; Garonna *et al.*, 2014). Previous large-scale studies have also mostly considered the Northern Hemisphere (as illustrated in Figure 1), despite contrasting indications about productivity trends in the Southern Hemisphere (SH) for the last decade (Zhao & Running, 2010) and despite the most commonly used sensor (AVHRR) having a global reach. In sum, the spatial and temporal coverage of existing large-scale LSP studies remains imbalanced, and the need for comprehensive global analyses of long-term changes in the seasonal patterns of VIs has already been recognized (Buitenwerf *et al.*, 2015).

In this paper, we evaluate the evolution and variability of Growing Season Length (GSL) over the past 30 years at global scale, based on an analysis of the most extensive (both in time and space) VI time series available to date. Our characterization of LSP trends of the last 30 years adds a decade to the most extensive global study in Figure 1 (Julien & Sobrino, 2009) and pursues two main objectives: (1) identify specific bioclimatic zones where LSP change has occurred; (2) evaluate the relative contribution of Start- and End- of Season (SOS and EOS, respectively) to the overall changes. Taking into consideration the available literature on the topic, our analysis seeks to provide consistent and comprehensive estimates of large-scale LSP trends over the last 3 decades, suitable for global studies.

MATERIAL AND METHODS

Two common descriptors of SOS, EOS and GSL were used to extract LSP metrics on annual and per-pixel bases. We examined the temporal variation of these metrics through the period 1982-2012 and interpreted existing trends using an independent global environmental stratification. This methodology is based on previous work at regional scale (Garonna *et al.*, 2014), which was further developed as described in the following sections.

Time series of vegetation activity

The $NDVI_{3g}$ dataset, generated from NOAA's Advanced Very High Resolution Radiometer (AVHRR) data and developed by NASA's Global Inventory Monitoring and Modelling Systems (GIMMS) group, is the longest continuous time series of vegetation activity presently available at global scale (Tucker *et al.*, 2005; Pinzon & Tucker, 2014). Two data points per month are provided at a 0.0833 degree spatial resolution. The estimated overall uncertainty is ±0.005 NDVI units throughout the AVHRR continuum (Pinzon & Tucker, 2014) and negligible in comparison to the minimum annual variation we imposed in our analysis (0.1 NDVI units). This latest version ($NDVI_{3g}$) was developed with the aim of providing a continuous and non-stationary global data record throughout the AVHRR timespan, which are particularly suitable for trend analysis (Zeng *et al.*, 2013; Pinzon & Tucker, 2014). $NDVI_{3g}$ has been recalibrated to improve data quality at Northern latitudes (Pinzon & Tucker, 2014).

Within the $NDVI_{3g}$ record, less than 0.01% of land pixels contain values flagged as 'missing data' within their time series. Data points flagged as 'possible snow', very common at northern high latitudes, were retrieved by Pinzon & Tucker (2014) either from the average seasonal profile or from spline interpolation. We considered these values as part of the LSP seasonality of snow-affected data, and therefore did not remove them from our time series. To correct for cloud interference, however, we used each year of $NDVI_{3g}$ data (1981-2012) as input for the Harmonic Analysis of NDVI Time Series (HANTS) algorithm (version 1.3, Fast Fourier implementation (Roerink *et al.*, 2000; Roerink *et al.*, 2003; de Wit & Su, 2005), which produces a smooth yearly curve using both Fourier analysis and an iterative flagging of outliers within the time series. We parameterized HANTS following (Garonna *et al.*, 2014). For the HANTS implementation as well as for all following steps, we considered calendar years (January to December) for Northern Hemisphere (NH) pixels and July-to-June NDVI time series for Southern Hemisphere (SH) pixels.

Extraction of LSP metrics

We used two commonly used definitions for SOS and EOS following White *et al.* (2009) and Garonna *et al.* (2014), which we call $Midpoint_{pixel}$ and Max-Increase methods (MP and MI, respectively). The MP method uses a relative threshold to define SOS: namely, SOS is the day-of-year at which the NDVI reaches half its annual amplitude in an upward direction. The MI method defines SOS as the day of maximum increase in NDVI in the year. For both MP and MI, the EOS is defined as the first day (after SOS) with an NDVI value lower or equal to the NDVI at SOS for that year. SOS and EOS are expressed in Day-Of-Year (DOY) and the GSL is the number of days between SOS and EOS within a year.

We adopted the algorithm used in Garonna *et al.* (2014) and added flags in order to better account for irregularities in the growing season and to identify various cases that required special attention. Each of these flags is summarized and described in Table 1. Each pixel having more than 15 flagged metrics (i.e. 50% of the total available years) was discarded from further analysis.

Analysis of temporal variability

For each pixel, we examined trends for GSL, SOS and EOS using linear regression, and tested the significance of a non-zero slope using a t-test. Only statistically significant trends at 5% level were considered in our results. In order to shed light on multi-decadal changes in LSP, we analysed the variability in the trends in global average GSL using a 10-year moving window. In order to compare our global trend estimates with previous global studies, we further tested for significance and extent of significant trends over the 1982-1991 and 1982-2003 periods. Moreover, for each GSL time series, we tested for the presence of a trend shift in the 31-year long time series by means of an F-test, which considers a potential single-shift of unknown timing in the time series (Andrews & Ploberger, 1994; Hansen, 2002; Andrews, 2003; Zeileis *et al.*, 2003). This method – illustrated in Figure 2 – uses an iterative procedure that minimizes the residual sum of squares to estimate the optimal break position within a specified data window. In our case, we assigned minimum segment length of 5 years before/after a breakpoint (corresponding to approximately 15% of the total time period), following suggestions of previous studies (Bai & Perron, 2003; Verbesselt *et al.*, 2010; de Jong *et al.*, 2012). Although time series may contain more than one significant trend shift, the F-test identifies only the most relevant shift in the time series (where it exists). Where evidence for structural change in the regression coefficients was found, its timing was dated using the method of (Zeileis *et al.*, 2003).

Environmental stratification

We used the Global Environmental Stratification (GEnS) to stratify our results (Metzger *et al.*, 2013b). This high-resolution bioclimate map of the Earth is available through the Group on Earth Observation (GEO) portal (http://www.geoportal.org). GEnS classifies all land areas in 125 strata, 18 environmental zones (GEnZ) and 7 biomes using multivariate statistical clustering (Metzger *et al.*, 2013a; Metzger *et al.*, 2013b). Its native resolution is 30 arcsec (approximately $1km^2$ at the equator) in the Winkel Tripel projection (Metzger *et al.*, 2013b). We rasterized and resampled GEnS to match the $NDVI_{3g}$ spatial resolution using a maximum area criterion (Verburg *et al.*, 2011). In other words, the class covering the largest area within a pixel determined the pixel class attribution. An implication of this aggregation method is that the overall representation of less prevalent classes is further reduced in the resampled data (Verburg *et al.*, 2011).

Examining the spatial distribution of the trends found, we considered a "hotspot" of LSP change any GEnS climatic zone with the highest proportion of significant GSL trends within it, as well as a good between-methods agreement both in terms of this proportion and in the average change estimates found (absolute difference < 0.1 days/year). To evaluate the area covered by the LSP changes found, we re-projected our results as well as the GEnS stratification to the equal-area MODIS Sinusoidal projection.

RESULTS

GSL climatology for 1982-2012

Our algorithm successfully captured SOS, EOS and GSL metrics from 71% of all land pixels available at GIMMS $NDVI_{3g}$ resolution (approximately 2 x 10^6 pixels in total), thus providing annual LSP metrics for most vegetated land areas. The remaining i.e. discarded areas were the following: pixels presenting no distinct NDVI seasonality and/or little vegetation cover represented 14% of all land pixels (in white in Figure 3); and pixels flagged as having two or more growing seasons during a year covered 15% of land pixels (in grey in Figure 3). The latter covered parts of the Amazon and central African forested areas, as well as most of Ethiopia and Somalia, Northern India, North-Eastern China, Northern Argentina and central United States.

Most of the NH presented both low Coefficient of Variation (CV) values (< 0.2) and a high proportion (>80%) of successful LSP metric extracted for each pixel from the 31 year-long $NDVI_{3g}$ time series (Figure 3) – indicating that the LSP metrics extracted were consistent in these regions. This was particularly true for roughly all areas > 40°N. Conversely, drylands and tropical biomes generally presented a low proportion of non-flagged observations as well as high year-to-year variability in GSL estimates (i.e. high CV values in Figure 3) and we considered these areas with particular caution in the interpretation of our results.

Trends in Growing Season Length (GSL) for 1982-2012

We found significant trends (α = 5%) in GSL over 13-19% of global land areas (as derived from MI and MP, respectively). The majority of areas presenting significant trends (63% for MP and 54% for MI) exhibited a lengthening of the growing season. Globally, our results indicate an average global lengthening of 0.34-0.22 days/year (according to MP and MI, respectively). Table 2 presents average estimates and extent of trends over the 1981-1991 period (following the Myneni *et al.* 1997 study) and over 1982-2003 period (as the Julien & Sobrino 2009 study), as well as over 1982-2012 (entire $NDVI_{3g}$ time series). We found good agreement between our $NDVI_{3g}$-derived trends and these two global studies listed in Figure 1. Differences in change estimate between time periods considered indicated a pattern of decreasing magnitude in GS lengthening with increasing timespan of the study. Conversely, the total area affected by GSL change approximately doubled when considering 1982-2012 as compared to the first decade only (Table 2).

Results from our structural change test suggested the vast majority of significant GSL trends are monotonic. Only 3% of all pixels with significant GSL change presented evidence of structural change: these were located mostly in Eastern Siberia and Northern Canada, where the most frequent timing of the estimated shifts in GSL were the early 2000s and the 1990s, respectively. However, analysing the variability in the trends of global average GSL using a 10-year moving time window, we observe a lower and even reversed trend in the 2000s, both using the MP and MI metrics.

GSL trends varied greatly with environmental zone (Figures 4 and 5). GS lengthening was found within the “Cold and Mesic” and “Cool, Temperate and Dry” zones spanning across boreal Eurasian and North America, as well as in a large part of the “Extremely Hot and Xeric” zone, particularly in the Sudano-Sahelian region and in large parts of India (Figure 4). On the other hand, GS shortening was found mostly in the “Extremely Cold and Mesic” zone across N. America and Siberia. Finally, shortening was also found in small strata in central Asia as well as in Northern Argentina, Southern Australia and North-Eastern China. Figure 5 presents both the average change estimates found per environmental zone (as derived from both methods), as well as the zonal distribution of the GSL trends found. We found greater disparity between methods in dry areas i.e. all zones qualified as "arid", "xeric" or "dry" and "extremely hot" areas, as opposed to "wet", "moist" and "mesic" zones which tended to have closer trend estimations. The MI method led to fewer significant trends overall, as well as higher trend averages per zone (Figure 5).

Significant GSL trends were found in each environmental zone and biome, but there was large variation is the area displaying change as well as in the magnitude of the trends found for each zone and biome. We found the "Boreal/Alpine" zone to contain the largest area of change found by both methods i.e. more than 1/3 of the total area. Within this biome, the "Cold and Mesic" zone – covering a long latitudinal belt around Eurasia and North American continents – stands out for its large area of change (approximately 20% of the total) – regardless of the method. Also, MI and MP methods agreed again on the strong positive GSL trend across this zone (on average, 0.73-0.8 days/year) as well as on the large proportion of this zone displaying significant trends (up to 37% of this zone, Figure 5). As such, the "Cold and Mesic" zone appeared as a 'hotspot' zone of GSL change.

Other zones displaying considerable areas of change (>10% of total) were: the "Extremely Cold and Mesic" zone – which showed GS shortening of up to 0.5 days/year across a wide area covering Pan-Arctic lands, and was characterized by an average shortening of the GSL of -0.32 and -0.47 days/year (MP and MI, respectively; Figure 5); the "Cool, Temperate and Dry" zone, the "Extremely Hot and Xeric" and the "Extremely Hot and Mesic" zone. All environmental zones mentioned are illustrated in Figure S4 in the Supplementary Online Materials (SOM) section.

Figure 6 illustrates the variation in mean GSL with time for the "Cold and Mesic" zone as well as for all land areas taken together. The MP and MI methods showed a very similar pattern in inter-annual GSL variation, with R-squared values of 0.82 and 0.91 for the "Cold and Mesic" and global times series (Figure 6). The between-method structural difference in global GSL estimates was 7.29±0.73 days, but was only of the order of ~1-2 days for both the "Cold and Mesic" zone (Figure 6).

Inter-annual variation and trends in SOS and EOS

Figure 7 presents the seasonal and inter-annual variation in global NDVI, SOS and EOS over the study period. Similarly to the overall GSL results (previous section), the year-to-year variations in SOS and EOS at global scale were consistent between MP and MI methods (Figures 6), although the MP method led to consistently later SOS than the MI method both in each environmental zone individually and globally (Figure 7 and Figure S5 in SOM). We found that, when averaged globally, both SOS and EOS underwent significant trends over 1982-2012 ($\alpha = 5\%$, Figure 7). The global EOS trend was stronger than the SOS equivalent: the global EOS delay was +0.22 / +0.26 days/year (MI and MP estimates, respectively), compared to -0.02 / -0.08 days/year of SOS change (Table 2).

The per-pixel distributions of SOS and EOS trends are presented in Figure 8. Regardless of the method used, we found significant advances in SOS over most of the boreal and continental Pan-Europe, parts of central Asia as well as central China (Figure 8a). On the other hand, significantly delayed SOS was found over parts of the mid-Western United States and in North-Eastern Argentina. Most of the Pan-Arctic showed an advanced EOS, whereas a delayed EOS was visible over most of the Northern boreal belt – mainly concentrated around the Baltic Sea, Eastern Canada and in the Sudano-Sahelian region (Figure 8b). EOS trends covered 13-21% of the land surface (MI and MP estimates, respectively), and were thus more widespread than SOS trends, which covered 9-14% of the land surface (MI and MP methods, respectively).

DISCUSSION

Examining the variability in the phenology of land surfaces globally and over the last 30+ years (as derived from $NDVI_{3g}$) reveals substantial spatial variation in GSL, SOS and EOS trends. Over 1/3 of areas with significant GSL change were found over the "Boreal/Alpine" biome. Yet within this biome are two environmental zones with contrasting GSL evolution. In the following discussion we examine more closely our findings and their implications, and highlight key areas for further research.

A global GSL climatology for 1982-2012

Numerous studies in the last decade have revealed a recent increase in carbon uptake by vegetated land areas (Schimel *et al.*, 2001; Poulter *et al.*, 2014; Sitch *et al.*, 2015), in parallel with marked vegetation 'greening' across vast areas of the Earth's surface (de Jong *et al.*, 2011). Our global study of LSP trends contributes to this field of research, in that it provides a recent climatology of intra-annual vegetation dynamics, consistently and at global scale. Indeed, the gradients of average GSL seen in Figure 3 reflect the spatial variation in the vegetation's seasonal carbon uptake.

We found both dryland and tropical biomes to have high year-to-year variability in GSL estimates throughout the study period (Figure 3). In tropical areas, however, the high variability in LSP metrics is unlikely to reflect actual land surface processes. Intense and persistent cloud cover together with dense canopies – where the NDVI signal saturates – are two characteristics of the evergreen tropics that may lead to irregular $NDVI_{3g}$ profiles and thus to the low proportion of LSP metrics successfully extracted over our 31-year-long study analysis (as seen in Figure 3). For drylands, however, the high GSL variability is in agreement with the findings of (Zhang *et al.*, 2014), who relate this to the high year-to-year variation in soil moisture as compared to temperature. Rainfall-driven systems tend to have much more variable phenological cycles (Hein *et al.*, 2011), as for instance in Australia, where shifts in peak timing of more than 1 month may be found (Broich *et al.*, 2014). High GSL inter-annual variability may thus indicate a moisture limitation of the vegetation.

Shifting global LSP dynamics

Our average GSL change estimates using $NDVI_{3g}$ were comparable with the two other global LSP studies using AVHRR data when considering the same time periods (Julien & Sobrino, 2009; Myneni et al., 1997; Table 2). Our GSL trend estimate for 1982-2012 represents a slower GS lengthening than indicated by previous (shorter-spanning) studies (Figures 1 and S1, Table 2). The multi-decadal differences in average GSL change estimate (Table 2) as well as the varying rate of global change found when performing a 10-year moving-window regression indicate that global GS lengthening has not occurred at a regular pace over the past three decades. In particular, the decreasing rate found in GS lengthening between the 1990s and the 2000s suggests that the 'global growing season' has lengthened, but at a decreasing rate. This indication evokes the slowing-down hypothesis previously put forward by Jeong *et al.* (2011) for SOS in temperate regions of the NH, whereby average GSL change estimates went from +0.56 days/year for 1982-1999 to +0.39 days/year for 2000-2008. Interestingly this appears to contrast with the results from our structural change tests: these qualified most GSL trends as monotonic and are in agreement with a recent study on shifts or abrupt changes in SOS, which also concluded that linear models were best suited to explain trends over most of the NH (Wang *et al.*, 2015). Further analyses at regional scale are needed to ascertain this aspect in view of seemingly contrasting indications from different sources. However, it is likely that the few observations (31 data points) available from the present observational record as well as the considerable year-to-year variability found in GSL estimates (Figure 3, Figure 6) are important hindrances to the statistical derivation of structural change in our LSP time series.

Understanding the relative contribution of shifting SOS and EOS towards the GSL trends found is a key first step towards the understanding of large-scale drivers of LSP variability. Given varying physical processes driving SOS and EOS, leaf phenology coupled to LSP corresponds better to vegetation greenness during SOS, while greenness is not an optimal predictor for EOS. Our results indicate that the overall GS lengthening for 1982-2012 may increasingly be attributed to an EOS delay. Long-term trends in EOS were both more extensive and stronger globally than those of SOS. This highlights the importance of shifting autumn events in studying large-scale phenological change, despite their being relatively understudied as compared to spring events (Gallinat *et al.*, 2015). The between- and within-species asynchrony in leaf senescence, the complex mix of drivers involved and the lack of a precise definition for EOS are some of the challenges involved in studying leaf senescence at large scales (Gallinat *et al.*, 2015; Panchen *et al.*, 2015). Indeed, amongst the LSP studies reviewed in Figure 1, only two (Julien & Sobrino, 2009; Jeong *et al.*, 2011) highlighted the important contribution of senescence timing to GSL changes at large scale. At regional or smaller-scale, studies have increasingly put forward the study of autumn leaf phenology as key for better explaining variations in productivity. For instance, a study using eddy covariance measurements reported that changes in autumn leaf phenology better explained the variation in annual net ecosystem productivity at Harvard Forest over 1992-2008 than spring phenology (Wu *et al.*, 2013). Following research efforts will examine attribution of LSP change to large-scale drivers at global scale, independently for SOS and EOS.

The "Boreal/Alpine": predominant biome of LSP change (1982-2012)

MP and MI showed good agreement on the spatial distribution of significant LSP trends – albeit with some differences in the average trend estimates (Table 2, Figures 5 and 6). Both methods found more than 1/3 of all trends found within the "Boreal/Alpine" biome of the Northern Hemisphere (NH). This distribution suggests that intra-annual vegetation dynamics are mirroring global warming over this period – which has been twice as fast as the global average in this region (IPCC, 2007; Scheffer *et al.*, 2012; IPCC, 2013). The consequences of these changes for the boreal carbon sink remain to be further studied. Indications are that the boreal (and arctic) carbon-climate feedbacks could be disproportionally large (Schimel *et al.*, 2015).

The fact that the "Boreal/Alpine" biome has relatively little anthropogenic presence and hence, direct pressure on vegetated lands (Ellis & Ramankutty, 2008) suggests that these LSP changes may be primarily climate-driven. Increased vegetation activity (i.e. greening), increasing air temperatures and reduced snow cover duration (Brown, 2000; Dye, 2002) have already been associated with a longer GS in these areas (Bogaert *et al.*, 2002; Alcaraz-Segura *et al.*, 2010). Undoubtedly snow cover duration plays a large role in this biome's LSP dynamics for two main reasons. Firstly, snow cover influences vegetation physiology and phenology through the micro-climate, soil hydrology and geochemistry (Walker *et al.*, 2001). Secondly, the reflectance of snow being very high at optical wavelengths (Pomeroy & Brun, 2001), the presence of numerous and repeated snow-affected satellite observations leads to a characteristic sharp rise/drop in NDVI at the first/last snow-free retrieval and make snow presence a major determinant of the land surface seasonality (Dye, 2002). For the "Boreal/Alpine" biome, 10% of the raw $NDVI_{3g}$ time series on average (1982-2012) were flagged as "possibly snow". We therefore consider shifts in snow cover duration as a probable main driving factor of LSP change in this biome. This is in agreement with a previous study comparing the spatial and temporal patterns among snow-cover and the NDVI trends in northern Eurasia (1982-1999), and linking the derived "greening" trends both to more favourable conditions for growth (through rising temperatures) and to declining snow-cover effects on NDVI (Dye & Tucker, 2003). A promising step forward for the study of vegetation dynamics in this region is the reconstruction of long-term AVHRR NDVI time series that aim to correct for the effect of confounding abiotic factors such as snow or bare soil, such as presented in (Zhang, 2015). However, the presence of snow within an AVHRR pixel does not rule out that vegetation may be active. It is therefore difficult to exclude snow contamination to some extent, particularly at large spatial scales and in a boreal biome.

Within the boreal biome, the "Cold and Mesic" and the "Extremely Cold and Mesic" environmental zones display the most significant large-scale changes in LSP (Figure S4). Interestingly, these two zones have contrasting average trends in GSL: the "Cold and Mesic" zone is where the most extensive rapid lengthening of the GS has occurred between 1982-2012; and the "Extremely Cold and Mesic" zone has undergone widespread shortening during the same period. On one hand, our results reveal the "Cold and Mesic" zone – covering broadly boreal forest areas at 50-65°N – as a hotspot of LSP change, because it encompasses the largest area of GSL change whilst displaying close agreement in the trend estimates found between methods (Figures 5 and 6). This has particular relevance in view of examining shifts in large-scale climatic phenological controls over this area, and testing the links between these observed LSP trends and their potential climatic drivers. Both SOS and EOS trends appear to contribute to this GS lengthening found, which we estimated at ~0.7 days/year on average. Trend estimates for this environmental zone relied on a full time series for the three decades i.e. no special flag appeared as illustrated in Figure 3, adding confidence to the idea that this region is a global hotspot of LSP change.

On the other hand, the boreal "Extremely Cold and Mesic" zone – showed an opposite overall trend in GSL over the period 1982-2012. Negative GS trends were widespread in this zone (Figure 4). However, different processes stand out between North America and Eurasia: whilst both SOS and EOS appear to have contributed to the negative GSL changes in North America, the East Siberian GSL trend appeared to be driven mostly by an earlier senescence (Figure 8). A recent small-scale study in Alaska highlighted that the increasingly abundant shrubs are transforming the landscape phenology of many tundra areas, and that these tend to have an earlier onset of senescence compared to evergreen/graminoid canopies (Sweet *et al.*, 2015). The "Extremely Cold and Mesic" zone is also where we found two large-scale structural change areas: Canada (in the 1990s) and Eastern Siberia (post-2000). These continental differences contribute to on-going discussions. Browning trends have been identified in boreal North America from a variety of VI datasets (e.g. $GIMMS_g$, $GIMMS_{3g}$, SeaWiFS, SPOT-VGT and MODIS in Guay *et al.* (2014), as well as greening trends in boreal Eurasia including Eastern Siberia (de Jong *et al.*, 2011; Dutrieux *et al.*, 2012; Guay *et al.*, 2014). (Chen *et al.*, 2014) identified a turning point in the late 1980s in North America, and (Buermann *et al.*, 2014) found that the accelerated summer warming without an accompanying increase in summer precipitation for the period 1970-2000 in Siberian boreal forest may have led to declining vegetation growth since the mid-1990s. The attribution of the Eastern Siberian GSL trend to an EOS change mostly appears to be in agreement with Barichivich *et al.* (2013), who found that the spring green-up has kept up with the pace of warming in Northern biomes (>45° N), whereas leaf senescence delay has not, because of limiting factors such as light and moisture.

It is unclear whether the (slow but significant) shortening of the GS we identified for the "Extremely Cold and Mesic" is linked to a shift to a negative response of vegetation growth to increasing temperatures from the mid-1990s onward, as suggested by Buermann *et* *al.* (2014); or to a cooling trend as identified over the last decade in western North America and Eurasia by both *in situ* and remotely-sensed temperature and sea ice extent data (Bhatt *et al.*, 2013); or to large-scale transformation of the landscape because of increasing deciduous shrubs. Overall, a number of co-occurring climatic and vegetation changes appear to be at play over this area and need to be further explored (Urban *et al.*, 2014; Park *et al.*, 2015). Overall, our results highlight LSP change in an area that is already an important research focus for climate change science. This is not only because of the magnitude of environmental changes occurring in boreal areas (IPCC, 2013) but also for the multiple atmosphere-biosphere feedbacks to be considered (Pearson et al., 2013). For instance, as thawed soils release greenhouse gases (Parmentier *et al.*, 2013) and as the albedo decreases with Arctic greening, studies have pointed to a potential switch of Pan-arctic tundra from a carbon sink to a carbon source.

Limitations and outlook

It is generally agreed that no method is consistently superior for deriving LSP metrics for global applications (Reed *et al.*, 2003; Atkinson *et al.*, 2012). We chose HANTS based on previous assessments showing its ability to represent the intra-annual variability of GIMMS NDVI data (de Jong *et al.*, 2011). An important known limitation to this algorithm is its weaker ability to reproduce abrupt NDVI rise/fall upon snow melt/fall compared to – for instance – a double logistic fit (Beck *et al.*, 2006). It is therefore important to state that our choice of a common and consistent approach for the entire globe comes at the cost of it not being equally adapted to all biomes. Given our indication of the “Boreal/Alpine” biome as a major region of LSP change, future studies focusing on this biome should take this limitation into account.

Finally, despite the usefulness of studying LSP trends for understanding phenological patterns consistently and a variety of scales, it is important to reiterate that vegetation phenology and land surface phenology remain related yet distinct. LSP incorporates the effects of soil and snow (Kathuroju *et al.*, 2007) as well as anthropogenic disturbance or fires (White *et al.*, 2009). Upscaling ground phenological information to an $NDVI_{3g}$ pixel footprint requires taking into account not only interspecific variation in phenological state – which may be important (Gill *et al.*, 2015; Panchen *et al.*, 2015), but also the influence of the entire landscape on the NDVI (Fisher *et al.*, 2006). That is why establishing a relationship between NDVI-derived metrics and plant-physiological events remains a challenge (D'Odorico *et al.*, 2015). Steps forward in this direction are important and on going, particularly through the development of webcam observation networks as well as through the upscaling of field observations to landscape level (Liang & Schwartz, 2009; Hufkens *et al.*, 2012).

ACKNOWLEDGEMENTS

The study has been conducted in the framework of the University of Zurich Research Priority Program on 'Global Change and Biodiversity' (URPP GCB). We thank Jim Tucker and the NASA GIMMS team for providing the $NDVI_{3g}$ data for this analysis. We are grateful for the support of the Functional Genomics Center Zurich (FGCZ) of the University of Zurich in processing the data. In particular, we thank M. Hakateyama, H. Rehrauer and K. Shimizu. We are grateful to B. Schmid for discussions on the methodology and the interpretation of our results, and for suggesting useful references for this manuscript. We thank G. Schaepman-Strub for discussions on phenology studies in the Pan-Arctic region.

REFERENCES

Alcaraz-Segura D, Chuvieco E, Epstein HE, Kasischke ES, Trishchenko A (2010) Debating the greening vs. browning of the North American boreal forest: differences between satellite datasets. *Global Change Biology*, **16**, 760-770.

Andrews DW, Ploberger W (1994) Optimal tests when a nuisance parameter is present only under the alternative. *Econometrica: Journal of the Econometric Society*, 1383-1414.

Andrews DWK (2003) Tests for parameter instability and structural change with unknown change point: A corrigendum. *Econometrica*, **71**, 395-397.

Arora VK, Boer GJ (2005) A parameterization of leaf phenology for the terrestrial ecosystem component of climate models. *Global Change Biology*, **11**, 39-59.

Atkinson PM, Jeganathan C, Dash J, Atzberger C (2012) Inter-comparison of four models for smoothing satellite sensor time-series data to estimate vegetation phenology. *Remote Sensing of Environment*, **123**, 400-417.

Bai J, Perron P (2003) Computation and analysis of multiple structural change models. *Journal of Applied Econometrics*, **18**, 1-22.

Barichivich J, Briffa KR, Myneni RB *et al.* (2013) Large-scale variations in the vegetation growing season and annual cycle of atmospheric CO2 at high northern latitudes from 1950 to 2011. *Global Change Biology*.

Beck PSA, Atzberger C, H√∏Gda KA, Johansen B, Skidmore AK (2006) Improved monitoring of vegetation dynamics at very high latitudes: A new method using MODIS NDVI. *Remote Sensing of Environment*, **100**, 321-334.

Bhatt US, Walker DA, Raynolds MK *et al.* (2013) Recent declines in warming and vegetation greening trends over pan-Arctic tundra. *Remote Sensing*, **5**, 4229-4254.

Bogaert J, Zhou L, Tucker CJ, Myneni RB, Ceulemans R (2002) Evidence for a persistent and extensive greening trend in Eurasia inferred from satellite vegetation index data. *Journal of Geophysical Research D: Atmospheres*, **107**, ACL 4-1 - ACL 4-14.

Broich M, Huete A, Tulbure MG *et al.* (2014) Land surface phenological response to decadal climate variability across Australia using satellite remote sensing. *Biogeosciences*, **11**, 5181-5198.

Brown RD (2000) Northern Hemisphere Snow Cover Variability and Change, 1915-1997. *Journal of Climate*, **13**, 2339-2355.

Buermann W, Parida B, Jung M, Macdonald GM, Tucker CJ, Reichstein M (2014) Recent shift in Eurasian boreal forest greening response may be associated with warmer and drier summers. *Geophysical Research Letters*, **41**, 2014GL059450.

Buitenwerf R, Rose L, Higgins SI (2015) Three decades of multi-dimensional change in global leaf phenology. *Nature Clim. Change*, **5**, 364-368.

Chen B, Xu G, Coops NC *et al.* (2014) Changes in vegetation photosynthetic activity trends across the Asia-Pacific region over the last three decades. *Remote Sensing of Environment,* **144**, 28-41.

Cleland EE, Chuine I, Menzel A, Mooney HA, Schwartz MD (2007) Shifting plant phenology in response to global change. *Trends in Ecology & Evolution,* **22**, 357-365.

D'odorico P, Gonsamo A, Gough CM *et al.* (2015) The match and mismatch between photosynthesis and land surface phenology of deciduous forests. *Agricultural and Forest Meteorology,* **214-215**, 25-38.

De Beurs K, Henebry GM (2010) Spatio-Temporal Statistical Methods for Modelling Land Surface Phenology. . In: *Phenological Research: methods for environmental and climate change analysis.* (eds Hudson IL, Keatley MR) pp Page. New York, Springer.

De Jong R, De Bruin S, De Wit A, Schaepman ME, Dent DL (2011) Analysis of monotonic greening and browning trends from global NDVI time-series. *Remote Sensing of Environment,* **115**, 692-702.

De Jong R, Verbesselt J, Schaepman ME, Bruin S (2012) Trend changes in global greening and browning: contribution of short-term trends to longer-term change. *Global Change Biology*.

De Wit AJW, Su B (2005) Deriving phenological indicators from SPOT-VGT data using the HANTS algorithm. In: *Proceedings of the 2nd international VEGETATION user conference; 1998-2004: 6 years of operational activities.* (eds Veroustraete F, Bartholomè E, Verstraeten WW) pp Page, Luxembourg, EC.

Dutrieux LP, Bartholomeus H, Herold M, Verbesselt J (2012) Relationships between declining summer sea ice, increasing temperatures and changing vegetation in the Siberian Arctic tundra from MODIS time series (2000-11). *Environmental Research Letters,* **7**.

Dye DG (2002) Variability and trends in the annual snow-cover cycle in Northern Hemisphere land areas, 1972-2000. *Hydrological Processes,* **16**, 3065-3077.

Dye DG, Tucker CJ (2003) Seasonality and trends of snow-cover, vegetation index, and temperature in northern Eurasia. *Geophysical Research Letters,* **30**, 58-51.

Ellis EC, Ramankutty N (2008) Putting people in the map: anthropogenic biomes of the world. *Frontiers in Ecology and the Environment,* **6**, 439-447.

Fisher JI, Mustard JF, Vadeboncoeur MA (2006) Green leaf phenology at Landsat resolution: Scaling from the field to the satellite. *Remote Sensing of Environment,* **100**, 265-279.

Gallinat AS, Primack RB, Wagner DL (2015) Autumn, the neglected season in climate change research. *Trends in Ecology & Evolution*.

Garonna I, De Jong R, De Wit AJW, Mücher CA, Schmid B, Schaepman ME (2014) Strong contribution of autumn phenology to changes in satellite-derived growing season length estimates across Europe (1982–2011). *Global Change Biology,* **20**, 3457-3470.

Gill AL, Gallinat AS, Sanders-Demott R, Rigden AJ, Short Gianotti DJ, Mantooth JA, Templer PH (2015) Changes in autumn senescence in northern hemisphere deciduous trees: a meta-analysis of autumn phenology studies. *Annals of Botany*.

Guay KC, Beck PSA, Berner LT, Goetz SJ, Baccini A, Buermann W (2014) Vegetation productivity patterns at high northern latitudes: a multi-sensor satellite data assessment. *Global Change Biology,* **20**, 3147-3158.

Hansen BE (2002) Tests for parameter instability in regreessions with I(1) processes. *Journal of Business and Economic Statistics,* **20**, 45-59.

Hein L, De Ridder N, Hiernaux P, Leemans R, De Wit A, Schaepman M (2011) Desertification in the Sahel: Towards better accounting for ecosystem dynamics in the interpretation of remote sensing images. *Journal of Arid Environments,* **75**, 1164-1172.

Hufkens K, Friedl M, Sonnentag O, Braswell BH, Milliman T, Richardson AD (2012) Linking near-surface and satellite remote sensing measurements of deciduous broadleaf forest phenology. *Remote Sensing of Environment,* **117**, 307-321.

Ibañez I, Primack RB, Miller-Rushing AJ *et al.* (2010) Forecasting phenology under global warming. *Philosophical transactions of the Royal Society of London. Series B, Biological sciences,* **365**, 3247-3260.

Ipcc (2007) Contribution of Working Groups I, II and III to the Fourth Assessment Report of the Intergovernmental Panel on Climate Change. In: *Climate Change 2007: Synthesis report.* (ed Core Writing Team P, R.K. And Reisinger, A. (Eds.)) pp Page, IPCC, Geneva, Switzerland.

Ipcc (2013) Climate Change 2013: The Physical Science Basis. Working Group I Contribution to the IPCC 5th Assessment Report - Changes to the Underlying Scientific/Technical Assessment. pp Page.

Jeganathan C, Dash J, Atkinson PM (2014) Remotely sensed trends in the phenology of northern high latitude terrestrial vegetation, controlling for land cover change and vegetation type. *Remote Sensing of Environment,* **143**, 154-170.

Jeong SJ, Ho CH, Gim HJ, Brown ME (2011) Phenology shifts at start vs. end of growing season in temperate vegetation over the Northern Hemisphere for the period 1982-2008. *Global Change Biology,* **17**, 2385-2399.

Julien Y, Sobrino J (2009) Global land surface phenology trends from GIMMS database. *International Journal of Remote Sensing,* **30**, 3495-3513.

Kathuroju N, White MA, Symanzik J, Schwartz MD, Powell JA, Nemani RR (2007) On the use of the advanced very high resolution radiometer for development of prognostic land surface phenology models. *Ecological Modelling,* **201**, 144-156.

Liang L, Schwartz MD (2009) Landscape phenology: An integrative approach to seasonal vegetation dynamics. *Landscape Ecology,* **24**, 465-472.

Metzger MJ, Brus DJ, Bunce RGH *et al.* (2013a) Environmental stratifications as the basis for national, European and global ecological monitoring. *Ecological Indicators,* **33**, 26-35.

Metzger MJ, Bunce RGH, Jongman RHG, Sayre R, Trabucco A, Zomer R (2013b) A high-resolution bioclimate map of the world: A unifying framework for global biodiversity research and monitoring. *Global Ecology and Biogeography*, **22**, 630-638.

Morisette JT, Richardson AD, Knapp AK *et al.* (2009) Tracking the rhythm of the seasons in the face of global change: Phenological research in the 21 st century. *Frontiers in Ecology and the Environment*, **7**, 253-260.

Myneni RB, Keeling CD, Tucker CJ, Asrar G, Nemani RR (1997) Increased plant growth in the northern high latitudes from 1981 to 1991. *Nature*, **386**, 698-702.

Panchen ZA, Primack RB, Gallinat AS, Nordt B, Stevens A-D, Du Y, Fahey R (2015) Substantial variation in leaf senescence times among 1360 temperate woody plant species: implications for phenology and ecosystem processes. *Annals of Botany*.

Park H, Jeong S-J, Ho C-H, Kim J, Brown ME, Schaepman ME (2015) Nonlinear response of vegetation green-up to local temperature variations in temperate and boreal forests in the Northern Hemisphere. *Remote Sensing of Environment*, **165**, 100-108.

Parmentier FJW, Christensen TR, Sørensen LL, Rysgaard S, Mcguire AD, Miller PA, Walker DA (2013) The impact of lower sea-ice extent on Arctic greenhouse-gas exchange. *Nature Climate Change*, **3**, 195-202.

Pearson RG, Phillips SJ, Loranty MM, Beck PSA, Damoulas T, Knight SJ, Goetz SJ (2013) Shifts in Arctic vegetation and associated feedbacks under climate change. *Nature Clim. Change*, **3**, 673-677.

Peñuelas J, Rutishauser T, Filella I (2009) Phenology feedbacks on climate change. *Science*, **324**, 887-888.

Pinzon J, Tucker C (2014) A Non-Stationary 1981-2012 AVHRR NDVI3g Time Series. *Remote Sensing*, **6**, 6929-6960.

Pomeroy J, Brun E (2001) Physical properties of snow. *Snow ecology*, 45-126.

Poulter B, Frank D, Ciais P *et al.* (2014) Contribution of semi-arid ecosystems to interannual variability of the global carbon cycle. *Nature*, **509**, 600-603.

Reed BC, Brown JF, Vanderzee D, Loveland TR, Merchant JW, Ohlen DO (1994) Measuring phenological variability from satellite imagery. *Journal of Vegetation Science*, **5**, 703-714.

Reed BC, White M, Brown JF (2003) Remote sensing phenology. In: *Phenology: An Integrative Environmental Science.* pp Page.

Richardson AD, Anderson RS, Arain MA *et al.* (2012) Terrestrial biosphere models need better representation of vegetation phenology: results from the North American Carbon Program Site Synthesis. *Global Change Biology*, **18**, 566-584.

Richardson AD, Keenan TF, Migliavacca M, Ryu Y, Sonnentag O, Toomey M (2013) Climate change, phenology, and phenological control of vegetation feedbacks to the climate system. *Agricultural and Forest Meteorology*, **169**, 156-173.

Roerink G, Menenti M, Soepboer W, Su Z (2003) Assessment of climate impact on vegetation dynamics by using remote sensing. *Physics and Chemistry of the Earth, Parts A/B/C,* **28**, 103-109.

Roerink G, Menenti M, Verhoef W (2000) Reconstructing cloudfree NDVI composites using Fourier analysis of time series. *International Journal of Remote Sensing,* **21**, 1911-1917.

Scheffer M, Hirota M, Holmgren M, Van Nes EH, Chapin Iii FS (2012) Thresholds for boreal biome transitions. *Proceedings of the National Academy of Sciences of the United States of America,* **109**, 21384-21389.

Schimel D, Pavlick R, Fisher JB *et al.* (2015) Observing terrestrial ecosystems and the carbon cycle from space. *Global Change Biology,* **21**, 1762-1776.

Schimel DS, House JI, Hibbard KA *et al.* (2001) Recent patterns and mechanisms of carbon exchange by terrestrial ecosystems. *Nature,* **414**, 169-172.

Sitch S, Friedlingstein P, Gruber N *et al.* (2015) Recent trends and drivers of regional sources and sinks of carbon dioxide. *Biogeosciences,* **12**, 653-679.

Sweet SK, Griffin KL, Steltzer H, Gough L, Boelman NT (2015) Greater deciduous shrub abundance extends tundra peak season and increases modeled net CO2 uptake. *Global Change Biology,* **21**, 2394-2409.

Tucker CJ, Pinzon JE, Brown ME *et al.* (2005) An extended AVHRR 8-km NDVI dataset compatible with MODIS and SPOT vegetation NDVI data. *International Journal of Remote Sensing,* **26**, 4485-4498.

Tucker CJ, Slayback DA, Pinzon JE, Los SO, Myneni RB, Taylor MG (2001) Higher northern latitude normalized difference vegetation index and growing season trends from 1982 to 1999. *International Journal of Biometeorology,* **45**, 184-190.

Urban M, Forkel M, Eberle J, Hüttich C, Schmullius C, Herold M (2014) Pan-Arctic Climate and Land Cover Trends Derived from Multi-Variate and Multi-Scale Analyses (1981-2012). *Remote Sensing,* **6**, 2296-2316.

Verbesselt J, Hyndman R, Newnham G, Culvenor D (2010) Detecting trend and seasonal changes in satellite image time series. *Remote Sensing of Environment,* **114**, 106-115.

Verburg PH, Neumann K, Nol L (2011) Challenges in using land use and land cover data for global change studies. *Global Change Biology,* **17**, 974-989.

Walker D, Billings W, De Molenaar J (2001) Snow-vegetation interactions in tundra environments. *Snow ecology*, 266-324.

Wang X, Piao S, Xu X, Ciais P, Macbean N, Myneni RB, Li L (2015) Has the advancing onset of spring vegetation green-up slowed down or changed abruptly over the last three decades? *Global Ecology and Biogeography*.

White MA, De Beurs KM, Didan K *et al.* (2009) Intercomparison, interpretation, and assessment of spring phenology in North America estimated from remote sensing for 1982-2006. *Global Change Biology,* **15**, 2335-2359.

Wu C, Gough CM, Chen JM, Gonsamo A (2013) Evidence of autumn phenology control on annual net ecosystem productivity in two temperate deciduous forests. *Ecological Engineering,* **60**, 88-95.

Zeileis A, Kleiber C, Krämer W, Hornik K (2003) Testing and dating of structural changes in practice. *Computational Statistics & Data Analysis,* **44**, 109-123.

Zeng F-W, Collatz G, Pinzon J, Ivanoff A (2013) Evaluating and Quantifying the Climate-Driven Interannual Variability in Global Inventory Modeling and Mapping Studies (GIMMS) Normalized Difference Vegetation Index (NDVI3g) at Global Scales. *Remote Sensing,* **5**, 3918-3950.

Zeng H, Jia G, Epstein H (2011) Recent changes in phenology over the northern high latitudes detected from multi-satellite data. *Environmental Research Letters,* **6**.

Zhang X (2015) Reconstruction of a complete global time series of daily vegetation index trajectory from long-term AVHRR data. *Remote Sensing of Environment,* **156**, 457-472.

Zhang X, Tan B, Yu Y (2014) Interannual variations and trends in global land surface phenology derived from enhanced vegetation index during 1982-2010. *International Journal of Biometeorology*.

Zhao J, Wang Y, Hashimoto H, Melton FS, Hiatt SH, Zhang H, Nemani RR (2012) The Variation of Land Surface Phenology From 1982 to 2006 Along the Appalachian Trail. *IEEE Transactions on Geoscience and Remote Sensing*.

Zhao M, Running SW (2010) Drought-Induced Reduction in Global Terrestrial Net Primary Production from 2000 Through 2009. *Science,* **329**, 940-943.

Zhu W, Tian H, Xu X, Pan Y, Chen G, Lin W (2012) Extension of the growing season due to delayed autumn over mid and high latitudes in North America during 1982-2006. *Global Ecology and Biogeography,* **21**, 260-271.

TABLES

Table 1: Summary of quality flags used in the LSP retrieval algorithm.

Flag type	Description	Consequence
Two or more growing seasons within a year	This flag is based on the number of consecutive days of the year with an NDVI above the midpoint. For a detailed description see Garonna *et al.* (2014)	LSP metric discarded from further analysis
No distinct seasonality	Annual NDVI range of 0.1 or less	
Little/no vegetation	30-year mean NDVI is 0.1 or less	
Growing season straddling the year end	When SOS and/or EOS occur within the first/last 15 days of the year	The following year of NDVI data is considered before restarting the LSP retrieval process

Table 2**: GSL trend estimates relative to two previous studies at global scale.**

Time period	**Average GSL trend (days per year)**		**Area covered by trends (in % of global land areas, MP/MI methods)**
	Reported in previous study	**This study (MP / MI methods)**	
1981-1991	+1.09 (Myneni et al., 1997)	+1.13 / +1.01*	8 / 7
1982-2003	+0.8 (Julien & Sobrino, 2009)	+0.61 / +0.67	14 / 10
1982-2012	-	+0.22 / +0.34	13 / 19

*= the closest available time period was used i.e. 1982-1991.

FIGURE CAPTIONS

Figure 1: Summary illustration of trend estimates in GSL, SOS and EOS (from top to bottom, respectively) as reported in latitudinal large-scale and long-term LSP studies. The scope of each study is represented by a rectangle within the temporal and spatial scope of the present study (1982-2012, global). Each rectangle delineates the time period and latitudinal extent considered by the study, and is coloured corresponding to the trend reported. NB: The list of studies represented in this figure is not exhaustive. We selected the examples closest to a global extent, which considered at least 10 years of data and which explicitly reported quantitative estimates for LSP change. A summary figure including results from the present study is presented in the Supplementary Online Material section (Figure S1). Key: 1: Wang *et al.* (2015); 2: Jeganathan *et al.* (2014); 3: Barichivich *et al.* (2013); 4: Jeong *et al.* (2011); 5: Zeng *et al.* (2011); 6: Julien & Sobrino (2009); 7: Tucker *et al.* (2001); 8: Myneni *et al.* (1997).

Figure 2: The top graph presents a sample GSL time series for 1982-2012, of a single pixel in Alaska (60.91° N, 157.58° W). The solid grey line represents the trend line under the assumption of monotonicity, whereas the dashed grey line detects a structural change in the linear regression in the year 2000. The bottom graph presents the F statistics for this time series, crossing the significant boundary line (dotted) and reaching a maximum in the year 2000.

Figure 3: Average (top, in days), Coefficient of Variation (middle, no unit) and proportion (bottom, in %) of GSL metrics successfully extracted over 1982-2012, using the MP method. White areas represent pixels flagged as having low NDVI annual range or long-term average; grey represents pixels flagged as displaying two or more growing seasons during single years. For the top panel, contour lines represent thresholds of 100, 150 and 200 days.

Figure 4: Average linear trends in GSL (in days/year) using the MP method, averaged by environmental stratum. Only significant trends ($\alpha = 5\%$) are considered. Environmental strata for which less than 20% of the area displayed significant trends are left white. The corresponding map as derived from the MI method is presented in Figure S2 in the SOM section. Also, the per-pixel distribution of GS lengthening and shortening is presented in Figure S3 in the SOM.

Figure 5: Average GSL trend and standard error (in days/year, top) and distribution of significant ($\alpha = 5\%$) GSL trends (in % of total area, bottom panel) by Global ENvironmental Zone (GEnZ), as derived by the MP and MI methods (in light and dark grey colour, respectively). Biome names are indicated at the top. Zones are abbreviated as follows: ECW1: “Extremely Cold And Wet 1”; ECW2: “Extremely Cold And Wet 2”; CW: “Cold

And Wet"; ECM: "Extremely Cold And Mesic"; CM: "Cold And Mesic"; CTD: "Cool Temperate And Dry"; CTX: "Cool Temperate And Xeric"; CTM: "Cool Temperate and Moist"; WTM: "Warm Temperate And Mesic"; WTX: "Warm Temperate And Xeric"; HM: "Hot And Mesic"; HD: "Hot And Dry"; HA: "Hot And Arid"; EHA: "Extremely Hot And Arid"; EHX: "Extremely Hot And Xeric"; EHM: "Extremely Hot And Moist". The two Arctic environmental zones were discarded from the figure because of missing LSP data.

Figure 6: Time series of average global $NDVI_{3g}$-derived Growing Season Length (GSL) for 1982-2012, using both MP and MI methods (solid and dashed lined, respectively), for the "Cold and Mesic" zone (top panel) and for all land areas ("Global", bottom panel).

Figure 7: Seasonal and inter-annual variability in NDVI, SOS and EOS for global land areas (left panel) and the "Cold and Mesic" zone (CM, right panel). Markers indicate yearly average SOS and EOS values and lines represent trends (significant at 5%), as derived from the MP (blue) and MI (red) methods. Contour lines indicate average NDVI values. Quantitative estimates for the average GSL trend are expressed at the top of each plot in days/year. Calendar years (January-to-June) are used for Northern Hemisphere pixels; June-to-July are used for Southern Hemisphere pixels.

Figure 8: Spatial distribution of SOS (a) and EOS (b) trends (significant at $\alpha = 0.05$) contributing to significant GS shortening (orange) and lengthening (green), using the MP method. The corresponding figure as derived from the MI method is presented in the SOM section (Figure S5).

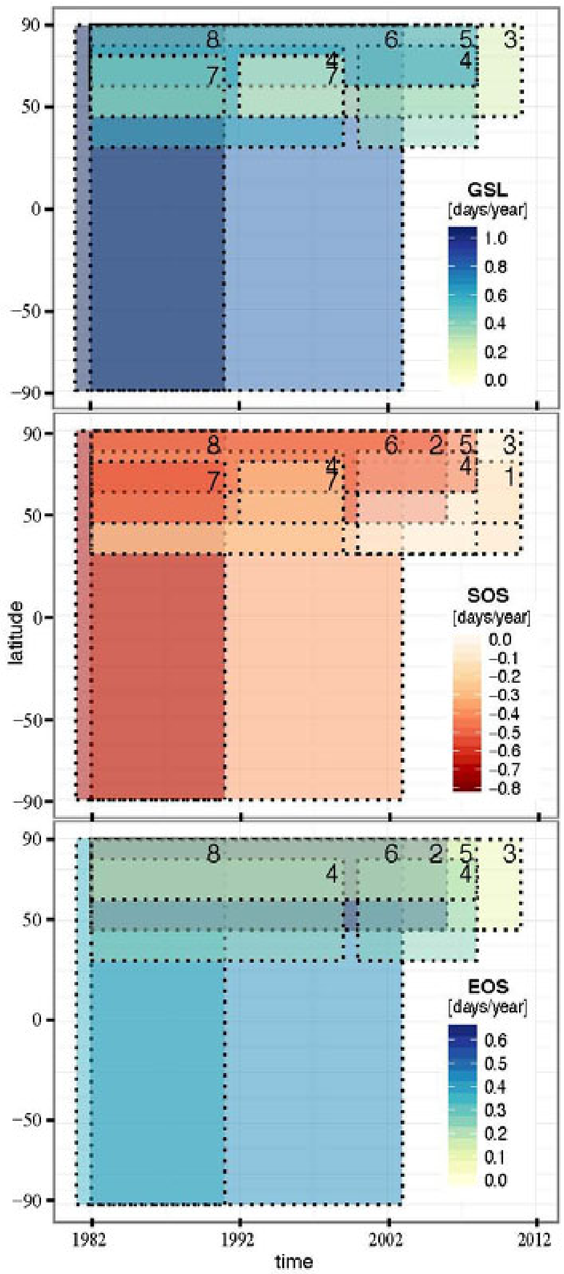
90
50
0
−50
−90
GSL
[days/year]
1.0
0.8
0.6
0.4
0.2
0.0
8
6
5
3
4
7
SOS
[days/year]
0.0
−0.1
−0.2
−0.3
−0.4
−0.5
−0.6
−0.7
−0.8
2
1
latitude
EOS
[days/year]
0.6
0.5
0.4
0.3
0.2
0.1
0.0
1982
1992
2002
2012
time

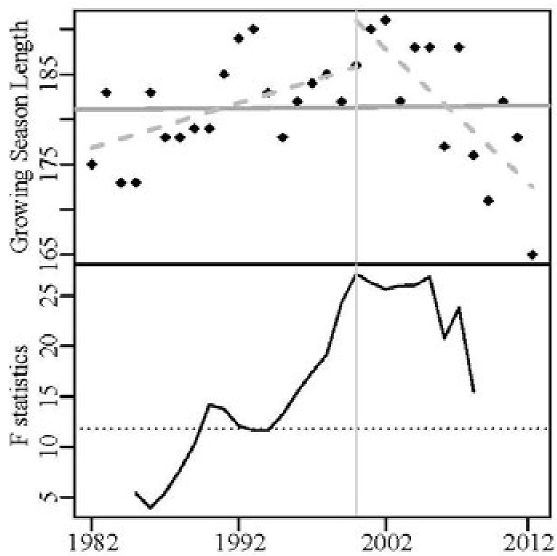
Growing Season Length
165
175
185
F statistics
5
10
15
20
25
1982
1992
2002
2012

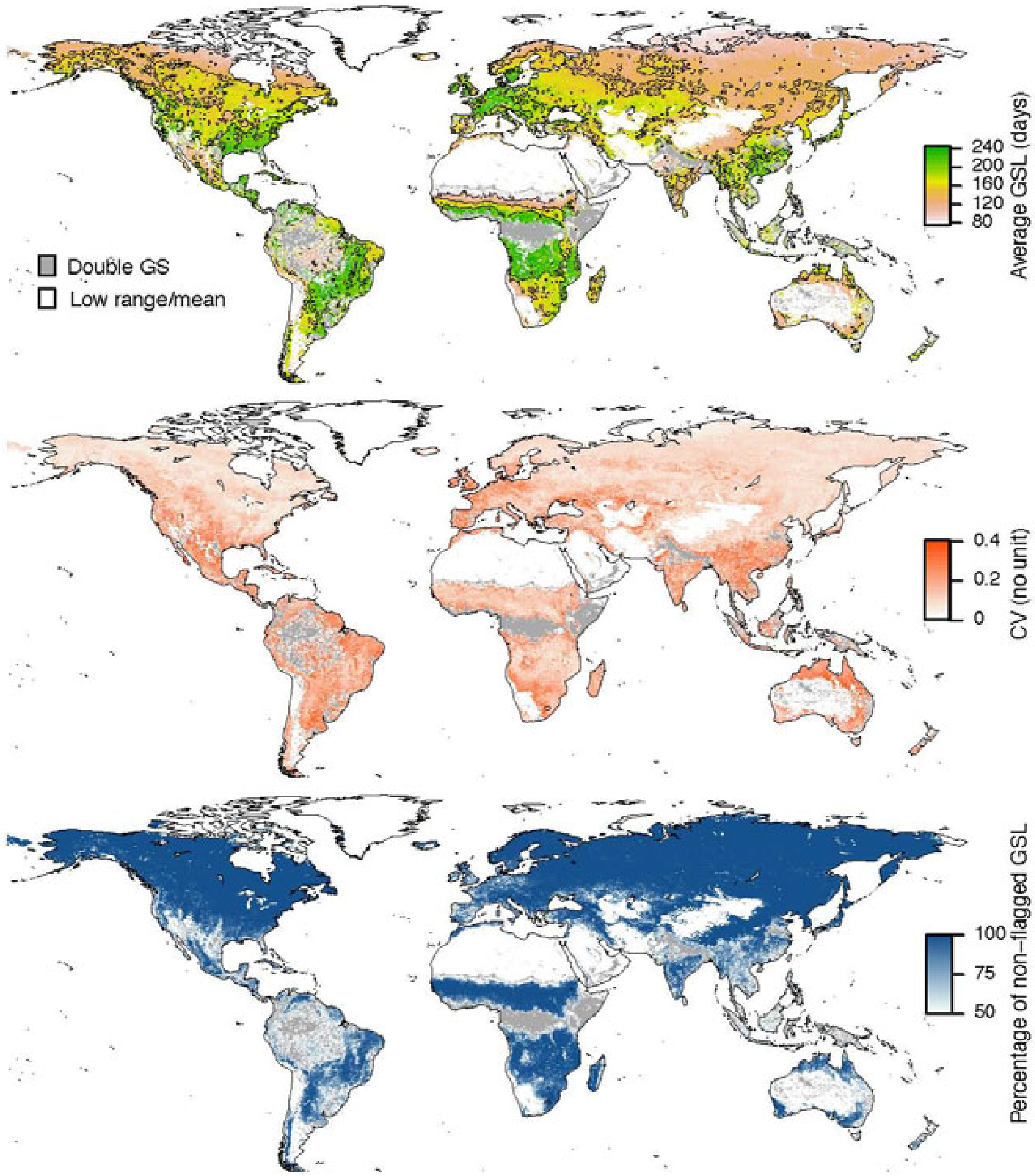
Double GS
Low range/mean
Average GSL (days)
240
200
160
120
80
CV (no unit)
0.4
0.2
0
Percentage of non-flagged GSL
100
75
50

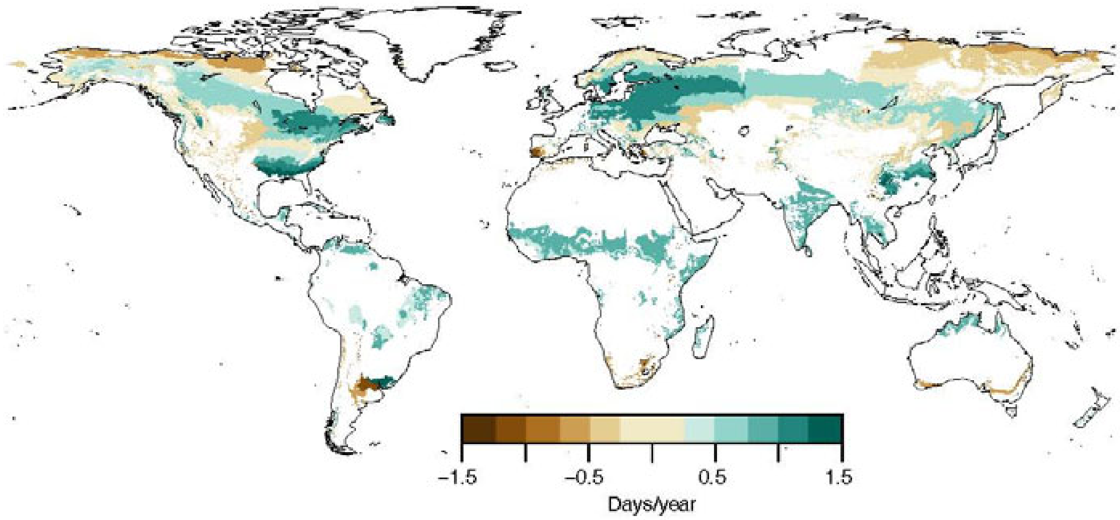
-1.5
-0.5
0.5
1.5
Days/year

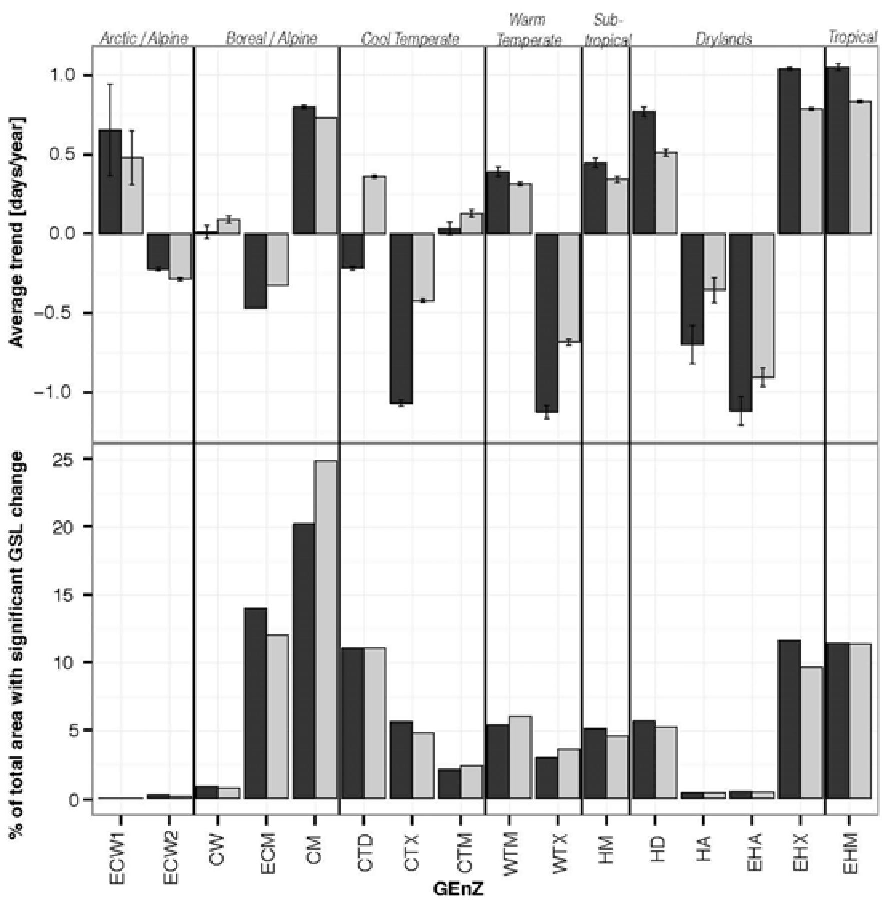
Arctic / Alpine
Boreal / Alpine
Cool Temperate
Warm Temperate
Sub-tropical
Drylands
Tropical
Average trend [days/year]
1.0
0.5
0.0
−0.5
−1.0
% of total area with significant GSL change
25
20
15
10
5
0
ECW1
ECW2
CW
ECM
CM
CTD
CTX
CTM
WTM
WTX
HM
HD
HA
EHA
EHX
EHM
GEnZ

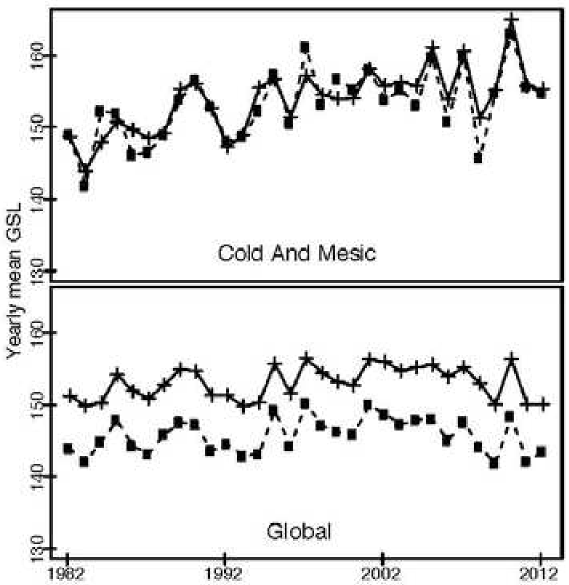
Yearly mean GSL
Cold And Mesic
Global
130
140
150
160
1982
1992
2002
2012

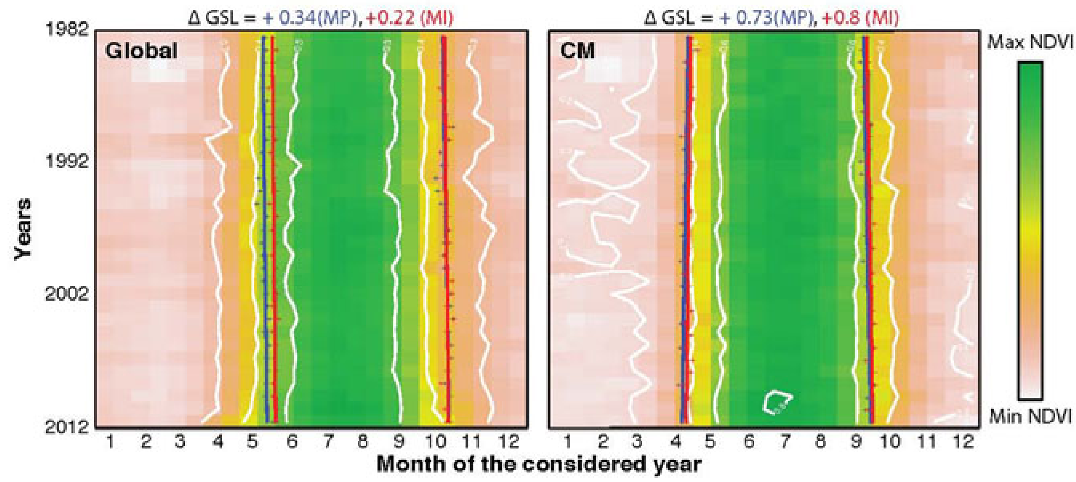
Δ GSL = + 0.34(MP), +0.22 (MI)
Δ GSL = + 0.73(MP), +0.8 (MI)
Global
CM
Max NDVI
Min NDVI
Years
1982
1992
2002
2012
1 2 3 4 5 6 7 8 9 10 11 12
Month of the considered year

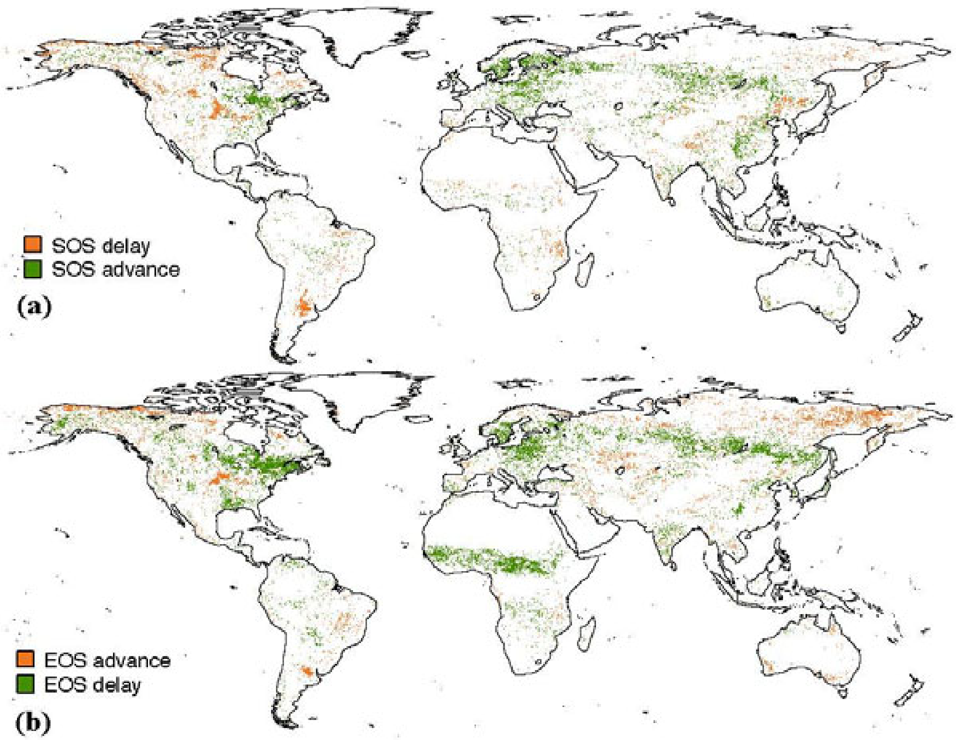
SOS delay
SOS advance
(a)
EOS advance
EOS delay
(b)